

Non-Leptonic Weak Decays of B to D_s and D mesons

C. E. Thomas*

Rudolf Peierls Centre for Theoretical Physics, University of Oxford,
1 Keble Road, Oxford, OX1 3NP

(Dated: 14 November 2005)

Branching ratios and polarisation amplitudes for B decaying to all allowed pseudoscalar, vector, axial-vector, scalar and tensor combinations of D_s and D mesons are calculated in the Isgur Scora Grinstein Wise (ISGW) quark model. We find good agreement with other models in the literature and the limited experimental data and make predictions for as yet unseen decay modes. Lattice QCD results in this area are very limited. We make phenomenological observations on decays in to $D_s(2317)$ and $D_s(2460)$ and propose tests for determining the status and mixings of the axial mesons.

PACS numbers: 13.25.Hw, 12.15.Ji, 12.39.Jh

I. INTRODUCTION

Non-leptonic weak decays of B-mesons are important because they probe both electroweak physics and hadronic structure, and may provide a window on physics beyond the standard model. As well as its intrinsic interest, the hadronic part must be understood in order to extract electroweak and new physics from these decays. This involves non-perturbative QCD and so can not be calculated from first principles. There have been many attempts to model the hadronic part and their success varies depending on which decay mode is studied. There are only very limited lattice QCD results in this area. Semi-leptonic decays of B and D mesons have been successfully studied using the Isgur Scora Grinstein Wise (ISGW) model [1]. We extend this model to the study of exclusive non-leptonic decays. The model has corrections that vanish when the final mesons have zero recoil and so should be most reliable close to this kinematic region.

Heavy Quark Effective Theory (HQET) as used, for example, in reference [2], provides a set of symmetry relations but not expressions for the rates. Some explicit model must still be used. The ISGW model satisfies the requirements of HQET in the zero recoil limit and provides an explicit model in which calculations can be made.

There are also pole models such as that of Bauer, Stech & Wirbel (BSW) [3][4] which we compare to our results. There are different approaches for heavy to light decays such as the Soft Collinear Effective Theory (SCET) framework [5] and Light-Cone Sum Rules [6][7]. These are useful where the final state mesons have high energy unlike the regime close to zero recoil that we are probing here.

Some predictions have been made for decays to combinations of pseudoscalar D_s and D and vector D_s^* and D* such as by Luo & Rosner [2] and Chen et. al. [8]. However, to our knowledge, there has been no extensive

study of decays to P-wave scalar, axial vector and tensor mesons. Datta and O'Donnell [9] have however made limited studies of the decays to axial and scalar D_s . With B factories tightening current observations of B decays and finding new decay modes it is timely that these modes should be studied in detail.

Our aims are to:

- Provide robust predictions of branching ratios and polarisation fractions for all the possible combinations. These can be compared with current and future experimental data
- Comment on what can be learnt about the nature of $D_s(2317)$ and $D_s(2460)$ mesons and axial vector mixing.

We start in Section II with a discussion of factorization and general remarks. In Section III we briefly describe the ISGW model and extend it to non-leptonic decays. In Section IV we present our results for the branching ratios and polarisation fractions of the allowed decay modes. We also compare our results with those from other models and experimental data in this section. In Section V we discuss what we can learn about the scalar and axial D_{s0} and D_{s1} . We finish with some general remarks and conclusions in Section VI and suggest some experimental observations that could be made.

II. GENERAL DEFINITIONS AND FACTORIZATION

The colour favoured tree diagram (“Type I tree diagram”) for $B \rightarrow D_s D$ is shown in Fig. 1. Here D_s and D can be any S or P-wave $s\bar{c}$ and $c\bar{u}$ states. We ignore any contribution to this process from penguin and weak-annihilation topologies.

The rate for a general Type I Tree decay $B(b\bar{q}_i) \rightarrow Y(q_1\bar{q}_2)X(q\bar{q}_i)$ (e.g. $Y = D_s$ and $X = D$) can be written as:

$$\Gamma = \frac{G_F^2}{16\pi} a_1^2 |V_{qb} V_{q_1 q_2}|^2 \frac{|\mathbf{q}|}{M_B^2} |A|^2. \quad (1)$$

*E-mail: c.thomas1@physics.ox.ac.uk

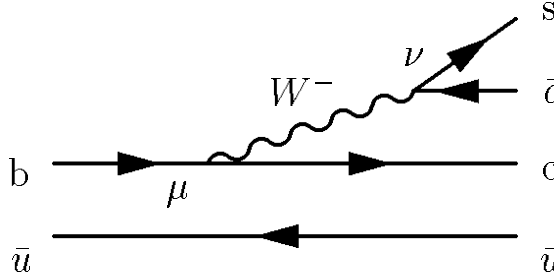


FIG. 1: $B^- (b\bar{u}) \rightarrow D_s^- (\bar{c}s) D^0 (c\bar{u})$ - Type I Tree Diagram

where G_F is the Fermi Constant, a_1 is the effective Wilson coefficient, V_{qb} and $V_{q_1 q_2}$ are CKM matrix elements, \mathbf{q} is the recoil 3-momentum in the rest frame of B and M_B is the B-meson mass. $|A|^2$ is the sum of the squares of the polarisation amplitudes A_i :

$$|A|^2 \equiv \sum_i |A_i|^2. \quad (2)$$

We use the notation $i = +-, -+$ or ll where the first label denotes the helicity of the X meson.

In QCD Factorization [10] [11] [12] in the heavy quark limit and to leading order in α_s the amplitude can be factorized as a product of two quark currents if weak annihilation contributions are ignored. Non-factorizable vertex, penguin and hard spectator corrections are incorporated in to the effective Wilson coefficients a_i . The coefficient a_1 varies from process to process but only by less than about 1%. It is therefore a good approximation to take one value, 1.05, for all processes [2]. The amplitude can therefore be written:

$$A_i = \langle Y | J_\mu | 0 \rangle \langle X | J^\mu | B \rangle, \quad (3)$$

where $J_\mu \equiv V_\mu - A_\mu \equiv \bar{q}_f \gamma_\mu (1 - \gamma_5) q_i$ is the vector-axial current.

The matrix element $\langle X | J^\mu | B \rangle$ can be parametrised in terms of general form factors. We use the same definitions as ISGW and these are given in Appendix A. These form factors can then be calculated in a particular model such as ISGW discussed in Section III. The polarisation vectors and tensors used for $J = 1$ and $J = 2$ mesons are given in Appendix B.

The matrix element $\langle Y | J_\mu | 0 \rangle$ can be parametrized in terms of the decay constant of meson Y , f_Y . For vector (3S_1) and axial vector (3P_1 , 1P_1) mesons [30] with polarisation vector ϵ_μ^Y and mass M_Y this is defined by

$$\langle Y | J_\mu | 0 \rangle = \epsilon_\mu^{*Y} f_Y M_Y, \quad (4)$$

and for scalar (3P_0) and pseudoscalar (1S_0) mesons [31]

with 4-momentum P_μ^Y ,

$$\langle Y | J_\mu | 0 \rangle = iP_\mu^Y f_Y. \quad (5)$$

III. THE ISGW MODEL

The ISGW model [1] was developed to calculate semileptonic B and D decays using a constituent quark model and the mock meson approach [13]. We extend the model to non-leptonic decays and test the sensitivity to the assumptions made. We find that robust predictions can be made for the $D_s D$ decay modes because they are in the valid kinematic region.

The matrix element $\langle X | J^\mu | B \rangle$ is calculated using a non-relativistic decomposition of the quark current $\bar{q} \gamma_\mu (1 - \gamma_5) b$. This will contain corrections of $O(|\mathbf{q}|^4/m_{q_i}^4)$ and $O(|\mathbf{q}|^4/M_X^4)$ where m_{q_i} are the quark masses appearing in the current decomposition. The model is therefore reliable only close to zero recoil and with heavy quarks. M_B is the mass of the B meson, M_X is the mass of the D (or excited D) meson, M_Y is the mass of the D_s (or excited D_s) meson. \tilde{M}_B , \tilde{M}_X and \tilde{M}_Y are the respective mock meson masses. P_B , P_X , P_Y are the 4-momenta, $y \equiv \frac{t}{M_B^2} = \frac{(P_B - P_X)^2}{M_B^2} = \frac{M_X^2}{M_B^2}$, and $t_m \equiv \max t = (M_B - M_X)^2$. The quarks are the spectator antiquark \bar{q}_i , the decaying quark b , the quark in the final state meson with the spectator quark q , and the quark and antiquark pair in the other final state meson q_1 and \bar{q}_2 . m_{q_i} , m_b , m_q , m_{q_1} and m_{q_2} are the constituent quark masses. In the decay $B^- \rightarrow D_s^- D^0$: $\bar{q}_i = \bar{u}$, $q = c$, $q_1 = s$ and $\bar{q}_2 = \bar{c}$.

In the original ISGW paper the semileptonic differential rate is given in terms of the form factors. We have adapted the model to calculate non-leptonic decays in the factorization hypothesis given above. The resulting relationships between polarisation amplitudes, form factors and decay constants are given in Appendix C. For connection with the original ISGW paper [1], their hadronic tensor (Equ. 7) is given by

$$h_{\mu\nu} = \sum_i \langle B | J_\nu^\dagger | X \rangle \langle X | J_\mu | B \rangle. \quad (6)$$

We initially followed the original ISGW paper using (radial ground state) harmonic oscillator (HO) wavefunction of the momentum space form:

$$\psi_{l=0, m_l=0}(\mathbf{k}) = (\pi \beta^2)^{-3/4} \exp\left(-\frac{|\mathbf{k}|^2}{2\beta^2}\right), \quad (7)$$

$$\psi_{l=1, m_l=0(1)}(\mathbf{k}) = \sqrt{2} (\pi \beta^2)^{-3/4} \frac{k_{z(+)}}{\beta} \exp\left(-\frac{|\mathbf{k}|^2}{2\beta^2}\right). \quad (8)$$

where β is the wavefunction parameter and $k_+ = -\frac{1}{\sqrt{2}}(k_x + ik_y)$. The wavefunctions are normalised such that $\int d^3k \psi^*(\mathbf{k}) \psi(\mathbf{k}) = 1$.

The resulting ISGW form factors using harmonic oscillator (HO) wavefunctions are given in Appendix D.

Quark	Constituent Quark Mass / MeV
b	5170
$q = c$	1770
$q_i = u$	330
$q_1 = c$	1770
$q_2 = s$	550

TABLE I: Constituent Quark Masses [14]

These are mostly the same as the ISGW paper but there are some modifications and additions which are explained in the appendix. The original ISGW paper was restricted to harmonic oscillator wavefunctions; our ISGW form factors for general wavefunctions are given in Appendix E.

In the original ISGW paper $|\mathbf{q}|^2$ in form factors is approximated as $(t_m - t)M_X/M_B$ and a relativistic correction factor κ is introduced through $|\mathbf{q}|^2 \rightarrow |\mathbf{q}|^2/\kappa^2$. This was intended to bring the pion form factor into better agreement with experiment at the low q^2 region [1]. We take $\kappa = 0.75$ [14]. However, we look at how much κ influences the results by setting $\kappa = 1$ in one model.

There is ambiguity in the mock meson approach [15] as to whether, at the end of the calculation, to identify the mock meson masses as the physical meson masses or the sum of the constituent quark masses.

We used a number of different models corresponding to different choices to assess the robustness of the approximations used. In model 1 the $(t_m - t)$ form is used in place of $|\mathbf{q}|^2$. In models 2 and 3 the exact $|\mathbf{q}|^2$ is used in the exponential of F_3 . In models 1-2 the mock meson masses are equal to the physical meson masses. In model 3 the physical meson masses are used except in the exponential of F_3 where the sum of the constituent quark masses is used. Models 4-5 take the mock meson masses to be the sum of the constituent quark masses. Model 4 uses $(t_m - t)$ and model 5 uses $|\mathbf{q}|^2$. Model 6 is the same as model 3 except that we set $\kappa = 1$.

The $D_s D$ decay mode is expected to be reasonably well modelled by ISGW. The highest recoil momentum (that for final state pseudoscalars) is 1812 MeV. $|\mathbf{q}|/m_b \approx 0.35$, $|\mathbf{q}|/m_c \approx 1.02$, $|\mathbf{q}|/M_D \approx 0.97$. Although $|\mathbf{q}|/m_c$ and $|\mathbf{q}|/M_D$ do not appear small, they appear as, for example, $|\mathbf{q}|^4/(8m_c^4)$, $|\mathbf{q}|^4/(8M_D^4)$ in a Taylor expansion with numerical value ≈ 0.14 . The approximation is therefore reasonable. In the following section we present the results of our calculation.

IV. RESULTS OF CALCULATION

Unless otherwise stated all numerical values of constants, masses etc. are taken from the PDG Review 2004 [19]. The quark masses and HO wavefunction parameters used are shown in Tables I and II respectively. We take $a_1 = 1.05$ [2], $|V_{bc}| = 0.04$ and $|V_{cs}| = 0.97$. The magni-

Meson	β / MeV
B	408
D	389
D^*	389
D_0	331
D_1	331
D_2	331

TABLE II: HO Wavefunction Parameters [16]

Meson	Decay Constant f / MeV
D_s	240 MeV [17]
D_s^*	275 MeV [17]
D_{s0}	110 MeV [18]
D_{s1} 1	233 MeV [18]
D_{s1} 2	87 MeV [18]

TABLE III: Decay Constants

tudes of decay constants used are given in Table III. The phases of the decay constants are chosen to match those given by quark model calculations in Appendix F.

We take the axial vector $D_{s1}(2460) \equiv D_{s1}$ to be 3P_1 and the $D_{s1}(2536) \equiv D_{s1}2$ to be 1P_1 . We take both axial D_1 to have mass 2420 MeV: D_{11} is 3P_1 and D_{12} is 1P_1 .

As discussed in Section III, to get a handle on the theoretical uncertainty within the ISGW model, we calculated the branching ratios and polarisation ratios using six different model choices.

A plot of the calculated decay rates and the experimental results is shown in Fig. 2. The model error bars and average show the range and average of the six model choices. The experimental results are from the PDG Review 2004 [19] except for the neutral B^0 decaying to $D_s^+ D^-$ which is taken from Belle [20]. Where data exist the model seems in remarkable agreement. The only possible exception is the new Belle result for the neutral B decay: $B^0 \rightarrow D_s^- D^+$. The variation due to the model choice is relatively small; it's of the same order or less than the experimental uncertainty for those modes with experimental data. This suggests the predictions made are robust. The model uncertainty shown does not include uncertainty in the decay constant: this would change the overall branching ratio for each Y (e.g. D_s) meson but not the pattern for a given Y .

The $D_{s1} D^*$, $D_{s1} D$ and $D_{s1}2 D^*$ modes are relatively large but are complicated by axial vector mixing. We comment on implications for D_{s0} and D_{s1} mesons in Section V.

Polarisation ratios for the relevant decay modes are shown in Fig. 3. There is only one piece of experimental data in the PDG Review 2004: that from BABAR and CLEO on the decay in to $D_s^* D^*$. Here there is reasonable model agreement. The model uncertainty is $\sim 10\%$

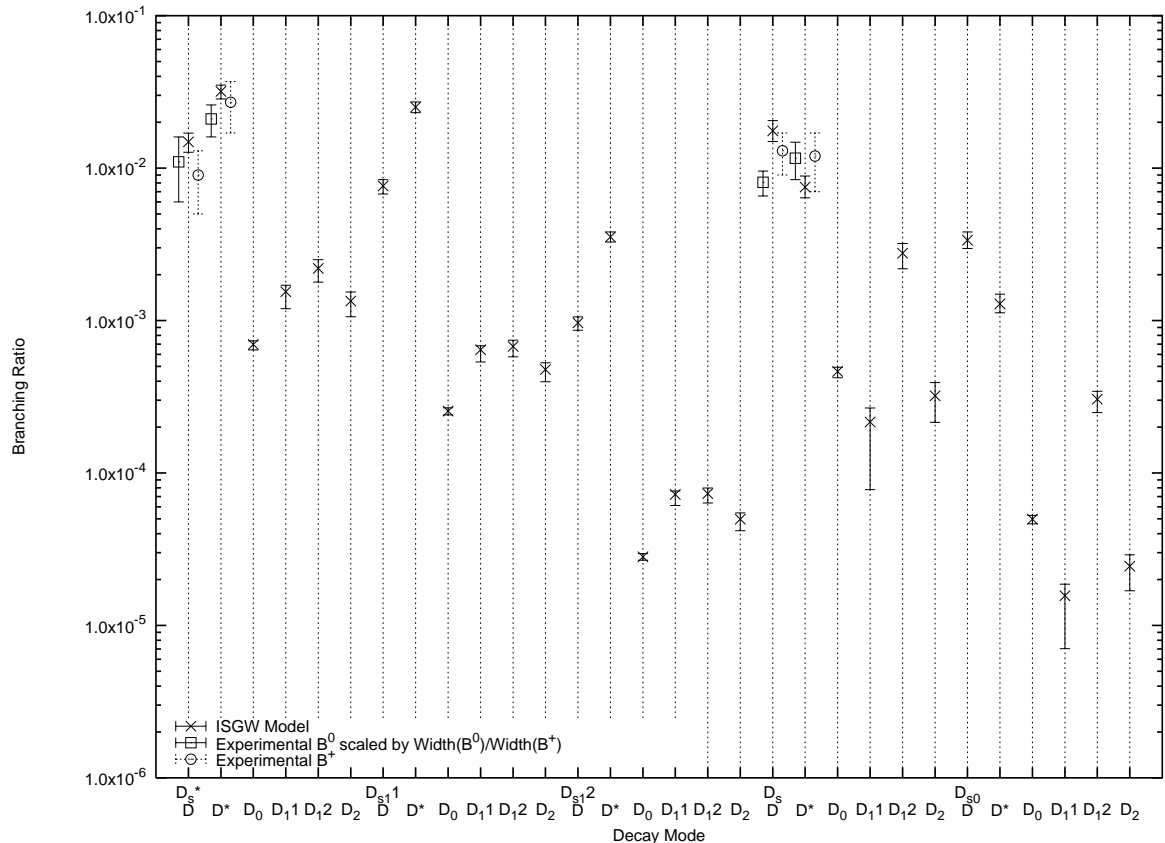


FIG. 2: $B \rightarrow D_s D$ Branching Ratios: ISGW model and experimental values

being slightly larger for the $D_1 1$ modes. Again the model

predictions are robust.

We compared these results with calculations based on the BSW model [3][4], Luo and Rosner's HQET based model in ref. [2] and the pole model in that reference. These models only allow predictions when meson X is a vector or pseudoscalar meson. The branching fraction results are shown in Fig. 4 and the polarisation ratios in Fig. 5. It can be seen that there is reasonably good agreement between the four models. This adds to our confidence in the robustness of our results. The ISGW model appears to give a slightly worse fit in some cases. However we should note that we haven't fitted anything to these decays. The only parameter, a_1 , was obtained for general B decays.

Lattice calculations currently only determine the form factors at zero recoil for semileptonic decays of B to D or D^* . Therefore branching ratios can not be compared with our calculations. For $B \rightarrow D$ the lattice results are given as $F(w=1)$ where $w = P_B \cdot P_X / (M_X M_B)$. This is related to the ISGW form factor f_+ by

$$F = \frac{2\sqrt{M_X M_B}}{M_X + M_B} f_+. \quad (9)$$

The ISGW model gives 0.961 to 1.02 depending on what masses are used for the mock meson masses. Lattice calculations give $1.074 \pm 0.018 \pm 0.016$ [21]. For $B \rightarrow D^*$ the lattice results are given as $F_A(w=1)$. This is related to the ISGW form factor f by

$$f = \sqrt{M_X M_B} F_A(w)(1+w). \quad (10)$$

The ISGW model gives this as 0.998 whereas a quenched lattice calculation gives $0.913^{+0.024} \pm 0.016^{+0.003+0.000+0.006} \pm 0.014-0.016-0.014$ [22]. In both cases the results of lattice and ISGW models differ.

We then looked at the ISGW model with more realistic wavefunctions using the results of Appendix E and a numerical solution of the radial Schrödinger equation. This was done by discretizing the position coordinate in to 300 intervals ranging from 0 to $1 - 2 \times 10^{-2} \text{ MeV}^{-1}$. We first checked our numerical method by solving a HO potential $V = 1/2\mu\omega^2 r^2$ where $\omega = \beta^2/\mu$ and μ is the reduced mass of the quarks. The results were the same as the HO analytic ones to the numerical accuracy.

We then used a more realistic Linear + Coulomb

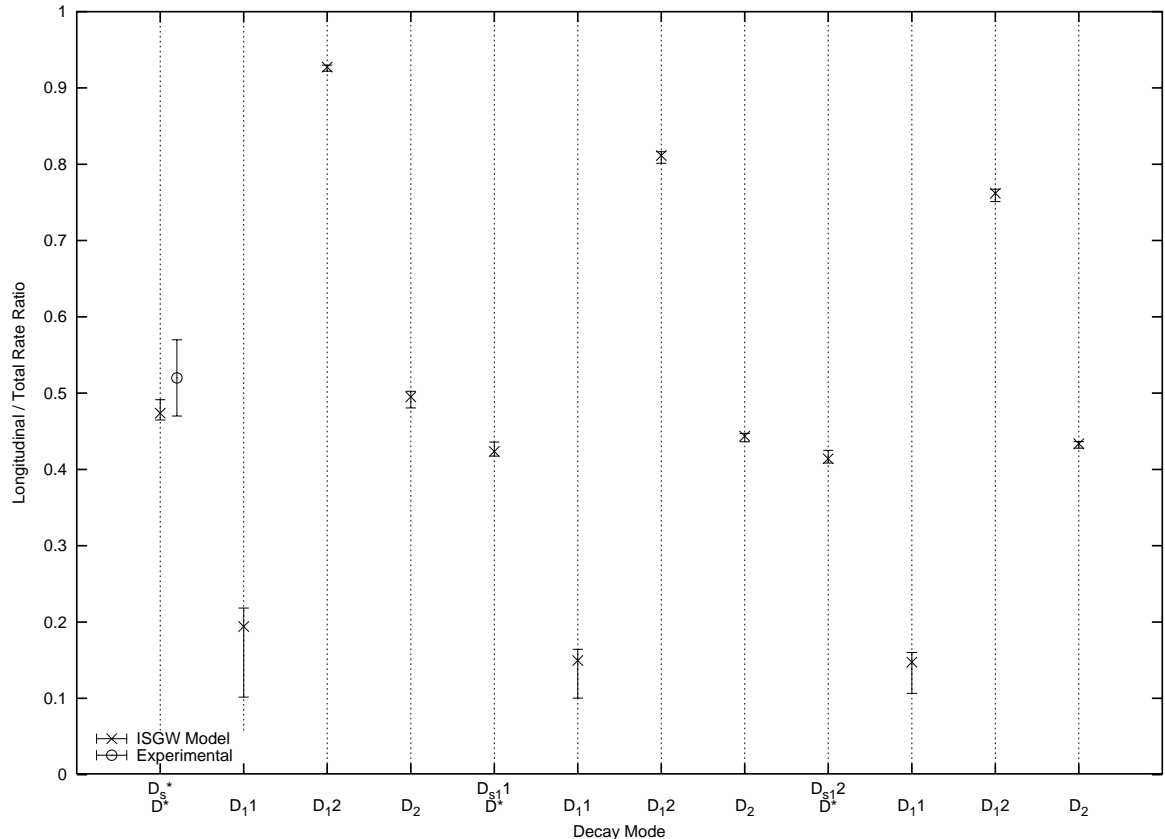


FIG. 3: Polarisation Ratios: ISGW model and experimental values

+ Hyperfine (LCHF) potential with the delta function smoothed out to a gaussian [23][24]:

$$V = -\frac{4 \alpha_s}{3 r} + br + \frac{32 \alpha_H \sigma^3}{9 m_q m_{\bar{q}} \sqrt{\pi}} (\mathbf{s}_q \cdot \mathbf{s}_{\bar{q}}) \exp(-\sigma^2 r^2). \quad (11)$$

Taking $\alpha_s = 0.594$, $b = 1.62 \times 10^5 \text{ MeV}^2$, $\sigma = 897 \text{ MeV}$ and $\alpha_H = \alpha_s$. The resulting form factors are negligibly different from the HO ones compared with the other model uncertainties. Varying the parameters in the LCHF potential by 10% leads to negligible changes in the results.

So, to summarize, the potential used does not appear to significantly modify our results.

V. PHENOMENOLOGICAL IMPLICATIONS FOR D_{s0} AND D_{s1}

The $D_s(2317)$ (0^+) and $D_s(2460)$ (1^+) do not fit easily in to the $c\bar{s}$ spectroscopy [25]. These states could be conventional $c\bar{s}$ mesons with lower than expected masses [26]. Alternatively they could be multiquark or molecular mesons associated with DK and D^*K thresholds [27]. Measuring branching ratios to D or D^* with $D_s(2317)$ and $D_s(2460)$ would help determine the nature of these mesons. If the measured branching ratios are consistent

with our predictions this would support them being conventional mesons. If this is the case, the mixing angle of the 3P_1 and 1P_1 states in to physical axial vector mesons $D_s(2460)$ and $D_s(2536)$ can also be determined.

In ref. [9] estimated experimental branching ratios are given for the $D_{s0} D$ as $\geq 10^{-3}$ and $D_{s1}(2460) D$ as $\leq 31.1 \times 10^{-4}$. The ISGW $D D_{s0}$ prediction is compatible with this estimate. The $D_{s1} D$ does not satisfy the experimental limit whereas the $D_{s1}2 D$ does. This is because we have ignored $^3P_1 - ^1P_1$ mixing. Datta and O'Donnell [9] claim that there is a discrepancy between experiment and theory. However they only consider ratios of decay constants and ignore the mass differences between the S and P-wave mesons. Here we have shown that if the ISGW model is used and the mass differences are taken in to account there is no inconsistency between experiment and theory.

Ignoring effects due to the different masses between the 3P_1 and 1P_1 axial vector mesons, the only difference in branching ratios is due to the decay constants. The quark model expressions for decay constants given in Appendix F imply that the branching ratio to $^3P_1 D_s$ is larger than that to $^1P_1 D_s$ because the first is proportional to the reduced mass whereas the later is proportional to the inverse of the difference of inverse masses. In the equal quark mass limit only the 3P_1 meson can be produced,

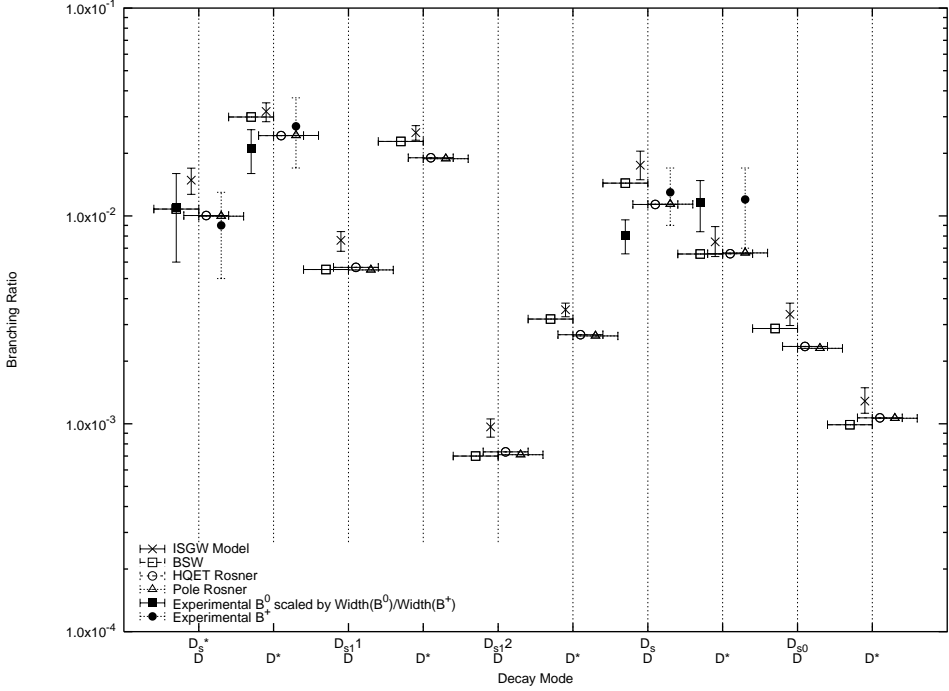
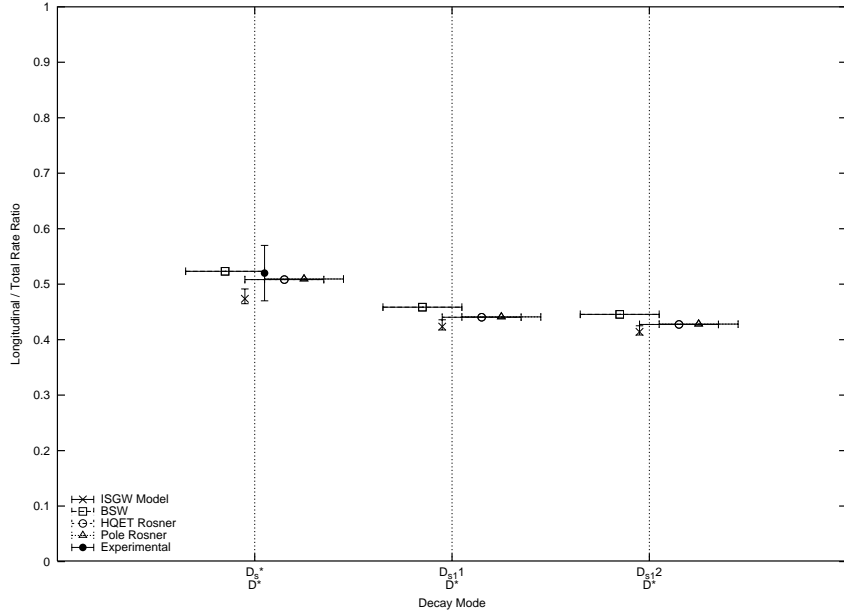
FIG. 4: $B \rightarrow D_s D$ Branching Ratios: Different models and experimental values

FIG. 5: Polarisation Ratios: Different models and experimental values

not the 1P_1 . In the heavy quark limit only the ${}^{1/2}1^+$ (jJ^P j-j coupling eigenstate) meson can be produced, not the ${}^{3/2}1^+$.

The axials and vectors can not be compared to the scalars and pseudoscalars as simply. This is because the amplitudes involve different combinations of form factors as seen in Appendix C.

VI. CONCLUSIONS

The ISGW model produces robust predictions for branching ratios and polarization fractions for the $B \rightarrow D_s D$ decays, which are in general agreement with the limited experimental data. The predictions are also in line with those from BSW, HQET and pole models. We have made predictions for all combinations of S and P-

wave final state mesons that can be measured in B decays. There are opportunities to probe the nature of the $D_s(2317)$ and $D_s(2460)$ states and determine the axial vector meson mixing using these decays. Measuring more polarisation fractions will be interesting because they weigh different form factors at the same momentum transfer. With the B factories at BABAR and Belle, CDF and later the LHCb, more precise data and also data on other decay modes should emerge.

It is important to note that these approximations are robust for the generic class of D_s D decays but are more suspect for $B \rightarrow J/\psi K$ (and excited) decays. These are outside the kinematically valid region and experimen-

tal data on these modes disagree with results from this model. Another possible contribution to these discrepancies could be final state rescattering of $(c\bar{s})$ $(u\bar{c})$ in to $(c\bar{c})$ $(u\bar{s})$ final states [28].

Acknowledgements

The initial idea for this work came from Frank Close and I thank Frank Close and Eric Swanson for useful discussions. This work was supported by a studentship from PPARC.

- [1] N. Isgur, D. Scora, B. Grinstein, and M. B. Wise, Phys. Rev. **D39**, 799 (1989).
- [2] Z. Luo and J. L. Rosner, Phys. Rev. **D64**, 094001 (2001), hep-ph/0101089.
- [3] M. Wirbel, B. Stech, and M. Bauer, Z. Phys. **C29**, 637 (1985).
- [4] M. Bauer, B. Stech, and M. Wirbel, Z. Phys. **C34**, 103 (1987).
- [5] C. W. Bauer, S. Fleming, D. Pirjol, and I. W. Stewart, Phys. Rev. **D63**, 114020 (2001), hep-ph/0011336.
- [6] V. L. Chernyak and I. R. Zhitnitsky, Nucl. Phys. **B345**, 137 (1990).
- [7] V. M. Belyaev, A. Khodjamirian, and R. Rückl, Z. Phys. **C60**, 349 (1993), hep-ph/9305348.
- [8] C.-H. Chen, C.-Q. Geng, and Z.-T. Wei, (2005), hep-ph/0507295.
- [9] A. Datta and P. J. O'Donnell, Phys. Lett. **B572**, 164 (2003), hep-ph/0307106.
- [10] M. Beneke, G. Buchalla, M. Neubert, and C. T. Sachrajda, Phys. Rev. Lett. **83**, 1914 (1999), hep-ph/9905312.
- [11] M. Beneke, G. Buchalla, M. Neubert, and C. T. Sachrajda, Nucl. Phys. **B591**, 313 (2000), hep-ph/0006124.
- [12] M. Beneke and M. Neubert, Nucl. Phys. **B675**, 333 (2003), hep-ph/0308039.
- [13] C. Hayne and N. Isgur, Phys. Rev. **D25**, 1944 (1982).
- [14] J. J. Dudek, *Phenomenology of Exotic Hadrons - Hybrid Mesons and Pentaquarks*, PhD thesis, Rudolf Peierls Centre for Theoretical Physics, Department of Physics, University of Oxford, 2004.
- [15] S. Capstick and S. Godfrey, Phys. Rev. **D41**, 2856 (1990).
- [16] F. E. Close and J. J. Dudek, Phys. Rev. **D69**, 034010 (2004), hep-ph/0308098.
- [17] M. Neubert and B. Stech, Adv. Ser. Direct. High Energy Phys. **15**, 294 (1998), hep-ph/9705292.
- [18] S. Veseli and I. Dunietz, Phys. Rev. **D54**, 6803 (1996), hep-ph/9607293.
- [19] Particle Data Group, S. Eidelman *et al.*, Phys. Lett. **B592**, 1 (2004).
- [20] K. Abe *et al.*, (2005), hep-ex/0508040.
- [21] M. Okamoto, (2005), hep-lat/0510113.
- [22] S. Hashimoto, A. S. Kronfeld, P. B. Mackenzie, S. M. Ryan, and J. N. Simone, Phys. Rev. **D66**, 014503 (2002), hep-ph/0110253.
- [23] E. S. Swanson, Ann. Phys. **220**, 73 (1992).
- [24] Private communication with Eric Swanson.
- [25] F. E. Close and E. S. Swanson, (2005), hep-ph/0505206.
- [26] W. A. Bardeen, E. J. Eichten, and C. T. Hill, Phys. Rev. **D68**, 054024 (2003), hep-ph/0305049.
- [27] T. Barnes, F. E. Close, and H. J. Lipkin, Phys. Rev. **D68**, 054006 (2003), hep-ph/0305025.
- [28] F. E. Close, E. S. Swanson, and C. E. Thomas, Paper in preparation.
- [29] A. Le Yaouanc, L. Oliver, O. Pene, and J. C. Raynal, Phys. Lett. **B387**, 582 (1996), hep-ph/9607300.
- [30] There are many definitions in the literature. Note that here we use the same conventions for vector and axial vector mesons.
- [31] Again there are many different conventions here. We use the same convention for scalar and pseudoscalar mesons.

APPENDIX A: GENERAL PARAMETRISATION OF VECTOR-AXIAL CURRENTS BETWEEN MESONS

When X is a pseudoscalar 1S_0 0^{-+} :

$$\langle X | V_\mu | B \rangle \equiv f_+(P_B + P_X)_\mu + f_-(P_B - P_X)_\mu. \quad (\text{A1})$$

When X is a vector 3S_1 1^{--} with polarisation vector ϵ_μ :

$$\langle X | A_\mu | B \rangle \equiv f\epsilon_\mu^* + a_+(\epsilon^* \cdot P_B)(P_B + P_X)_\mu + a_-(\epsilon^* \cdot P_B)(P_B - P_X)_\mu, \quad (\text{A2})$$

$$\langle X | V_\mu | B \rangle \equiv i g \epsilon_{\mu\nu\rho\sigma} \epsilon^{*\nu} (P_B + P_X)^\rho (P_B - P_X)^\sigma. \quad (\text{A3})$$

When X is a scalar 3P_0 0^{++} :

$$\langle X | A_\mu | B \rangle \equiv u_+ (P_B + P_X)_\mu + u_- (P_B - P_X)_\mu. \quad (\text{A4})$$

When X is an axial vector 3P_1 1^{++} with polarisation vector ϵ_μ :

$$\langle X | V_\mu | B \rangle \equiv l \epsilon_\mu^* + c_+ (\epsilon^* \cdot P_B) (P_B + P_X)_\mu + c_- (\epsilon^* \cdot P_B) (P_B - P_X)_\mu, \quad (\text{A5})$$

$$\langle X | A_\mu | B \rangle \equiv i q \epsilon_{\mu\nu\rho\sigma} \epsilon^{*\nu} (P_B + P_X)^\rho (P_B - P_X)^\sigma. \quad (\text{A6})$$

When X is an axial vector 1P_1 1^{+-} with polarisation vector ϵ_μ :

$$\langle X | V_\mu | B \rangle \equiv r \epsilon_\mu^* + s_+ (\epsilon^* \cdot P_B) (P_B + P_X)_\mu + s_- (\epsilon^* \cdot P_B) (P_B - P_X)_\mu, \quad (\text{A7})$$

$$\langle X | A_\mu | B \rangle \equiv i v \epsilon_{\mu\nu\rho\sigma} \epsilon^{*\nu} (P_B + P_X)^\rho (P_B - P_X)^\sigma, \quad (\text{A8})$$

When X is a tensor 3P_2 2^{++} with polarisation tensor $\epsilon_{\mu\nu}$:

$$\langle X | A_\mu | B \rangle \equiv k \epsilon_{\mu\nu}^* P_B^\nu + b_+ (\epsilon_{\alpha\beta}^* P_B^\alpha P_B^\beta) (P_B + P_X)_\mu + b_- (\epsilon_{\alpha\beta}^* P_B^\alpha P_B^\beta) (P_B - P_X)_\mu, \quad (\text{A9})$$

$$\langle X | V_\mu | B \rangle \equiv i h \epsilon_{\mu\nu\lambda\rho} \epsilon^{*\nu\alpha} P_{B\alpha} (P_B + P_X)^\lambda (P_B - P_X)^\rho. \quad (\text{A10})$$

APPENDIX B: POLARISATION VECTORS FOR $J = 1$ AND $J = 2$ MESONS

For a vector meson with 4-momentum $(E, 0, 0, |\mathbf{q}|)$ and mass M the polarisation vectors are

$$\epsilon_+^\mu = -\frac{1}{\sqrt{2}}(0, 1, i, 0), \quad (\text{B1})$$

$$\epsilon_-^\mu = \frac{1}{\sqrt{2}}(0, 1, -i, 0), \quad (\text{B2})$$

$$\epsilon_L^\mu = \frac{1}{M}(|\mathbf{q}|, 0, 0, E). \quad (\text{B3})$$

For a vector meson with 4-momentum $(E, 0, 0, -|\mathbf{q}|)$ and mass M the polarisation vectors (in the spin rather than the helicity basis) are

$$\epsilon_+^\mu = -\frac{1}{\sqrt{2}}(0, 1, i, 0), \quad (\text{B4})$$

$$\epsilon_-^\mu = \frac{1}{\sqrt{2}}(0, 1, -i, 0), \quad (\text{B5})$$

$$\epsilon_L^\mu = \frac{1}{M}(-|\mathbf{q}|, 0, 0, E). \quad (\text{B6})$$

For a tensor meson with 4-momentum $(E, 0, 0, |\mathbf{q}|)$ and mass M the polarisation tensors can be obtained by taking the outer product of two spin-1 polarisation vectors

with the appropriate Clebsh-Gordon coefficients. The polarisation tensors are given by:

$$\epsilon_{++}^{\mu\nu} = \frac{1}{2} \begin{bmatrix} 0 & 0 & 0 & 0 \\ 0 & 1 & i & 0 \\ 0 & i & -1 & 0 \\ 0 & 0 & 0 & 0 \end{bmatrix}, \quad (\text{B7})$$

$$\epsilon_+^{\mu\nu} = -\frac{1}{2M} \begin{bmatrix} 0 & |\mathbf{q}| & i|\mathbf{q}| & 0 \\ |\mathbf{q}| & 0 & 0 & E \\ i|\mathbf{q}| & 0 & 0 & iE \\ 0 & E & iE & 0 \end{bmatrix}, \quad (\text{B8})$$

$$\epsilon_0^{\mu\nu} = \sqrt{\frac{2}{3}} \begin{bmatrix} \frac{|\mathbf{q}|^2}{M^2} & 0 & 0 & \frac{|\mathbf{q}|E}{M^2} \\ 0 & -\frac{1}{2} & 0 & 0 \\ 0 & 0 & -\frac{1}{2} & 0 \\ \frac{|\mathbf{q}|E}{M^2} & 0 & 0 & \frac{E^2}{M^2} \end{bmatrix}, \quad (\text{B9})$$

$$\epsilon_-^{\mu\nu} = \frac{1}{2M} \begin{bmatrix} 0 & |\mathbf{q}| & -i|\mathbf{q}| & 0 \\ |\mathbf{q}| & 0 & 0 & E \\ -i|\mathbf{q}| & 0 & 0 & -iE \\ 0 & E & -iE & 0 \end{bmatrix}, \quad (\text{B10})$$

$$\epsilon_{--}^{\mu\nu} = \frac{1}{2} \begin{bmatrix} 0 & 0 & 0 & 0 \\ 0 & 1 & -i & 0 \\ 0 & -i & -1 & 0 \\ 0 & 0 & 0 & 0 \end{bmatrix}. \quad (\text{B11})$$

APPENDIX C: POLARISATION AMPLITUDES IN TERMS OF FORM FACTORS

For a pseudoscalar B decaying to a pseudoscalar (X) and a pseudoscalar (Y) the amplitude is given by

$$A = if_Y [(M_B^2 - M_X^2) f_+ + M_Y^2 f_-]. \quad (\text{C1})$$

For a decay in to a vector (X) and a pseudoscalar (Y) only a longitudinal vector is allowed and the amplitude is given by

$$A_L = -i \frac{f_Y |\mathbf{q}| M_B}{M_X} [f + a_+ (M_B^2 - M_X^2) + a_- M_Y^2]. \quad (\text{C2})$$

For a decay in to a pseudoscalar (X) and a vector (Y) only a longitudinal vector is allowed and the amplitude is given by

$$A_L = -2f_Y f_+ |\mathbf{q}| M_B. \quad (\text{C3})$$

For a decay in to a vector (X) and a vector (Y) the polarisations amplitudes for X positive, negative and longitudinal polarisation respectively are

$$A_{+-} = -f_Y M_Y (f + 2g|\mathbf{q}| M_B), \quad (\text{C4})$$

$$A_{-+} = -f_Y M_Y (f - 2g|\mathbf{q}| M_B), \quad (\text{C5})$$

$$A_{ll} = \frac{f_Y}{M_X} \left[f \left(|\mathbf{q}|^2 + \frac{1}{4M_B^2} (M_B^2 + M_X^2 - M_Y^2)(M_B^2 + M_Y^2 - M_X^2) \right) + 2a_+ |\mathbf{q}|^2 M_B^2 \right], \quad (\text{C6})$$

$$= \frac{f_Y}{M_X} [f P_Y \cdot P_X + 2a_+ |\mathbf{q}|^2 M_B^2]. \quad (\text{C7})$$

For a decay in to a tensor (X) and a pseudoscalar (Y) only a longitudinally polarised tensor is allowed and the amplitude is given by

$$A_L = -if_Y [k + b_+ (M_B^2 - M_X^2) + b_- M_Y^2] \sqrt{\frac{2}{3}} \frac{M_B^2 |\mathbf{q}|^2}{M_X^2}. \quad (\text{C8})$$

For a decay in to a tensor (X) and a vector (Y) the tensor can not have polarisation ± 2 . The polarisation amplitudes for X positive, negative and longitudinally polarised respectively are given by

$$A_{+-} = -f_Y \frac{M_B |\mathbf{q}| M_Y}{M_X \sqrt{2}} (k + 2h M_B |\mathbf{q}|), \quad (\text{C9})$$

$$A_{-+} = -f_Y \frac{M_B |\mathbf{q}| M_Y}{M_X \sqrt{2}} (k - 2h M_B |\mathbf{q}|), \quad (\text{C10})$$

$$A_{ll} = \sqrt{\frac{2}{3}} \frac{|\mathbf{q}| M_B f_Y}{M_X^2} \left[k \left(|\mathbf{q}|^2 + \frac{1}{4M_B^2} (M_B^2 + M_X^2 - M_Y^2)(M_B^2 + M_Y^2 - M_X^2) \right) + 2M_B^2 |\mathbf{q}|^2 b_+ \right]. \quad (\text{C11})$$

From these expressions it can be seen that the parity violation arises from a non-zero form factors g and h .

Amplitudes for when Y is an axial vector or scalar can be obtained simply by using the correct decay constant. Amplitudes when X is an axial vector or scalar can be obtained by replacing the vector or pseudoscalar form factors by the analogous axial or scalar ones given in Appendix A and multiplying by -1 to account for the difference in sign of the vector and axial currents in $V-A$.

APPENDIX D: ISGW FORM FACTORS FOR HARMONIC OSCILLATOR WAVEFUNCTIONS

We define:

$$\beta_{BX}^2 \equiv \frac{1}{2}(\beta_B^2 + \beta_X^2), \quad (D1)$$

$$\mu_{\pm} \equiv \left(\frac{1}{m_q} \pm \frac{1}{m_b} \right)^{-1}, \quad (D2)$$

and

$$F_n = \sqrt{\frac{\tilde{M}_X}{M_B}} \left(\frac{\beta_B \beta_X}{\beta_{BX}^2} \right)^{n/2} \exp \left[- \left(\frac{m_{qi}^2}{4\tilde{M}_X \tilde{M}_B} \right) \frac{t_m - t}{\kappa^2 \beta_{BX}^2} \right]. \quad (D3)$$

The pseudoscalar (1S_0) form factors are

$$f_+ = F_3 \left[1 + \frac{m_b}{2\mu_-} - \frac{m_b m_q m_{qi} \beta_B^2}{4\mu_+ \mu_- \tilde{M}_X \beta_{BX}^2} \right], \quad (D4)$$

$$f_- = F_3 \left[1 - (\tilde{M}_X + \tilde{M}_B) \left(\frac{1}{2m_q} - \frac{m_{qi} \beta_B^2}{4\mu_+ \tilde{M}_X \beta_{BX}^2} \right) \right]. \quad (D5)$$

The vector (3S_1) form factors are

$$f = 2\tilde{M}_B F_3 \quad (D6)$$

$$g = \frac{1}{2} F_3 \left[\frac{1}{m_q} - \frac{m_{qi} \beta_B^2}{2\mu_- \tilde{M}_X \beta_{BX}^2} \right], \quad (D7)$$

$$a_+ = -\frac{F_3}{2\tilde{M}_X} \left[1 + \frac{m_{qi}}{m_b} \left(\frac{\beta_B^2 - \beta_X^2}{\beta_B^2 + \beta_X^2} \right) - \frac{m_{qi}^2 \beta_X^4}{4\mu_- \tilde{M}_B \beta_{BX}^4} \right], \quad (D8)$$

$$a_- = \frac{F_3}{2\tilde{M}_X} \left[1 - \frac{\tilde{M}_X}{M_B} + \frac{\tilde{M}_X^2}{m_q \tilde{M}_B} - \frac{\beta_B^2 m_{qi} \tilde{M}_X}{2\beta_{BX}^2 M_B \mu_+} \right]. \quad (D9)$$

The axial vector (1P_1) form factors are

$$r = F_5 \frac{\tilde{M}_B \beta_B}{\sqrt{2}\mu_+}, \quad (D10)$$

$$v = F_5 \frac{\beta_B}{4\sqrt{2}m_b m_q}, \quad (D11)$$

$$s_+ = F_5 \frac{m_{qi}}{\sqrt{2}\tilde{M}_B \beta_B} \left[1 + \frac{m_b}{2\mu_-} - \frac{m_b m_q m_{qi} \beta_B^2}{4\mu_+ \mu_- \tilde{M}_X \beta_{BX}^2} \right], \quad (D12)$$

$$s_- = F_5 \frac{m_{qi}}{\sqrt{2}M_B \beta_B} \left[1 - \frac{\tilde{M}_X + \tilde{M}_B}{2m_q} + \frac{(\tilde{M}_X + \tilde{M}_B) \beta_B^2 m_{qi}}{4\mu_+ \beta_{BX}^2 \tilde{M}_X} \right]. \quad (D13)$$

Note the difference in v compared with B43 of [1], we have checked this and believe our expression is correct.

The scalar (3P_0) form factors are

$$u_+ = -F_5 \frac{m_b m_q m_{qi}}{\sqrt{6}\beta_B \tilde{M}_X \mu_-}, \quad (D14)$$

$$u_- = F_5 \frac{m_{qi}(\tilde{M}_X + \tilde{M}_B)}{\sqrt{6}\beta_B \tilde{M}_X}. \quad (D15)$$

Note the negative sign in u_+ compared with that in equation B37 of [1]. We think this is due to the Clebsh Gordon coefficient convention used.

The axial vector (3P_1) form factors are

$$q = F_5 \frac{m_{qi}}{2\tilde{M}_X \beta_B}, \quad (D16)$$

$$l = -F_5 \beta_B \tilde{M}_B \left[\frac{1}{\mu_-} + \frac{m_{qi}(t_m - t)}{2\tilde{M}_B \beta_B^2 \kappa^2} \left(\frac{1}{m_q} - \frac{m_{qi} \beta_B^2}{2\beta_{BX} \tilde{M}_X \mu_-} \right) \right], \quad (D17)$$

$$c_+ = F_5 \frac{m_{qi} m_b}{4\tilde{M}_B \beta_B \mu_-} \left[1 - \frac{m_{qi} m_q \beta_B^2}{2\tilde{M}_X \mu_- \beta_{BX}^2} \right], \quad (D18)$$

$$c_- = -F_5 \frac{m_{qi}(\tilde{M}_B + \tilde{M}_X)}{4\tilde{M}_B \beta_B} \left[\frac{1}{m_q} - \frac{m_{qi} \beta_B^2}{2\mu_- \beta_{BX}^2 \tilde{M}_X} \right]. \quad (D19)$$

The tensor (3P_2) form factors are

$$h = F_5 \frac{m_{qi}}{2\sqrt{2}M_B\beta_B} \left[\frac{1}{m_q} - \frac{m_{qi}\beta_B^2}{2\tilde{M}_X\mu_-\beta_{BX}^2} \right], \quad (\text{D20})$$

$$k = \sqrt{2}F_5 \frac{m_{qi}}{\beta_B}, \quad (\text{D21})$$

$$b_+ = -F_5 \frac{m_{qi}}{2\sqrt{2}\tilde{M}_X m_b \beta_B} \left[1 - \frac{m_{qi}m_b\beta_X^2}{2\mu_+\tilde{M}_B\beta_{BX}^2} + \frac{m_{qi}m_b\beta_X^2}{4\tilde{M}_B\mu_-\beta_{BX}^2} \left(1 - \frac{m_{qi}\beta_X^2}{2\tilde{M}_B\beta_{BX}^2} \right) \right], \quad (\text{D22})$$

$$b_- = F_5 \frac{m_{qi}}{2\sqrt{2}M_B^2\beta_B} \left[-1 + \frac{\tilde{M}_X}{m_q} + \frac{\tilde{M}_B}{\tilde{M}_X} - \frac{m_{qi}}{\mu_+} + \frac{m_{qi}(\tilde{M}_X + \tilde{M}_B)}{2m_b m_q} \right]. \quad (\text{D23})$$

APPENDIX E: ISGW FORM FACTORS FOR GENERAL WAVEFUNCTIONS

We define:

$$\beta_{BX}^2 \equiv \frac{1}{2}(\beta_B^2 + \beta_X^2), \quad (\text{E1})$$

and

$$\mu_\pm \equiv \left(\frac{1}{m_q} \pm \frac{1}{m_b} \right)^{-1} \quad (\text{E2})$$

In the following $\langle \rangle \equiv \langle X | B \rangle$ and $\langle O \rangle \equiv \langle X | O | B \rangle$. For example $\langle p_z \rangle = k \int d^3p \cdot p_z \cdot \psi^*(p) \psi(p)$. For notational convenience we include the common $\sqrt{\tilde{M}_X/\tilde{M}_B}$ factors in $\langle \rangle$ and $\langle O \rangle$.

The pseudoscalar (1S_0) form factors are

$$f_+ = \langle \rangle \left(1 + \frac{m_b}{2\mu_-} \right) + \frac{\langle p_z \rangle}{|\mathbf{q}|} \frac{m_b m_q}{2\mu_- \mu_+}, \quad (\text{E3})$$

$$f_- = \langle \rangle \left(1 - \frac{\tilde{M}_X + \tilde{M}_B}{2m_q} \right) - \frac{\langle p_z \rangle}{|\mathbf{q}|} \frac{\tilde{M}_X + \tilde{M}_B}{2\mu_+}. \quad (\text{E4})$$

The vector (3S_1) form factors are

$$g = \frac{1}{2} \left[\frac{\langle \rangle}{m_q} + \frac{\langle p_z \rangle}{|\mathbf{q}| \mu_-} \right], \quad (\text{E5})$$

$$f = 2 \langle \rangle \tilde{M}_B, \quad (\text{E6})$$

$$a_+ = -\frac{1}{2\tilde{M}_X} \left[\langle \rangle \left(1 + \frac{\tilde{M}_X}{M_B} - \frac{\tilde{M}_X^2}{m_q M_B} \right) - \frac{\langle p_z \rangle}{|\mathbf{q}|} \frac{\tilde{M}_X^2}{M_B \mu_+} \right], \quad (\text{E7})$$

$$a_- = \frac{1}{2\tilde{M}_X} \left[\langle \rangle \left(1 - \frac{\tilde{M}_X}{M_B} + \frac{\tilde{M}_X^2}{m_q M_B} \right) + \frac{\langle p_z \rangle}{|\mathbf{q}|} \frac{\tilde{M}_X^2}{M_B \mu_+} \right]. \quad (\text{E8})$$

The axial vector (1P_1) form factors are

$$r = \langle p_+ \rangle \frac{\tilde{M}_B}{\mu_+}, \quad (\text{E9})$$

$$v = \langle p_+ \rangle \frac{1}{4m_b m_q}, \quad (\text{E10})$$

$$s_+ = \langle \rangle \frac{M_X}{|\mathbf{q}| M_B} \left(1 + \frac{m_b}{2\mu_-} \right) + \langle p_z \rangle \frac{m_b m_q \tilde{M}_X}{2\tilde{M}_B \mu_+ |\mathbf{q}|^2 \mu_-} - \langle p_+ \rangle \frac{1}{2\tilde{M}_B \mu_+} \left(1 + \frac{m_b m_q \tilde{M}_X}{\mu_- |\mathbf{q}|^2} + \frac{m_b m_q}{2\mu_- M_X} \right), \quad (\text{E11})$$

$$s_- = \langle \rangle \frac{M_X}{|\mathbf{q}| M_B} \left(1 - \frac{(\tilde{M}_X + \tilde{M}_B)}{2m_q} \right) - \langle p_z \rangle \frac{\tilde{M}_X (\tilde{M}_X + \tilde{M}_B)}{2\tilde{M}_B \mu_+ |\mathbf{q}|^2} + \langle p_+ \rangle \frac{(\tilde{M}_X + \tilde{M}_B) \tilde{M}_X}{2\tilde{M}_B \mu_+ |\mathbf{q}|^2}. \quad (\text{E12})$$

The scalar (3P_0) form factors are

$$u_+ = -\langle \rangle \frac{1}{\sqrt{3}} \frac{m_b m_q}{|\mathbf{q}| \mu_-}, \quad (\text{E13})$$

$$u_- = \langle \rangle \frac{1}{\sqrt{3}} \frac{(\tilde{M}_X + \tilde{M}_B)}{|\mathbf{q}|}. \quad (\text{E14})$$

The axial vector (3P_1) form factors are

$$q = \langle \rangle \frac{1}{\sqrt{2}|\mathbf{q}|}, \quad (\text{E15})$$

$$l = -\frac{\tilde{M}_B}{\sqrt{2}} \left[\frac{\langle p_z \rangle}{\mu_-} + \frac{\langle \mathbf{q} \rangle}{m_q} + \frac{\langle p_+ \rangle}{\mu_-} \right], \quad (\text{E16})$$

$$c_+ = \frac{m_b m_q \tilde{M}_X}{2\sqrt{2}\tilde{M}_B |\mathbf{q}|^2 \mu_-} \left[-\frac{\langle p_+ \rangle}{\mu_-} + \frac{\langle p_z \rangle}{\mu_-} + \frac{\langle \mathbf{q} \rangle}{m_q} \right], \quad (\text{E17})$$

$$c_- = \frac{\tilde{M}_X (\tilde{M}_X + \tilde{M}_B)}{2\sqrt{2}\tilde{M}_B |\mathbf{q}|^2} \left[\frac{\langle p_+ \rangle}{\mu_-} - \frac{\langle p_z \rangle}{\mu_-} - \frac{\langle \mathbf{q} \rangle}{m_q} \right]. \quad (\text{E18})$$

The tensor $(^3P_2)$ form factors are

$$k = \langle \rangle \frac{2\tilde{M}_X}{|\mathbf{q}|}, \quad (\text{E19})$$

$$h = \frac{\tilde{M}_X}{2\tilde{M}_B |\mathbf{q}|^2} \left[\frac{\langle p_z \rangle}{\mu_-} + \frac{\langle \mathbf{q} \rangle}{m_q} - \frac{\langle p_+ \rangle}{\mu_-} \right], \quad (\text{E20})$$

$$b_+ = \frac{\tilde{M}_X^2}{2|\mathbf{q}|^2 \tilde{M}_B^2} \left[\langle p_z \rangle \left(\frac{1}{\mu_+} + \frac{1}{2\mu_-} \right) - \langle p_+ \rangle \left(\frac{1}{\mu_+} + \frac{1}{2\mu_-} \right) + |\mathbf{q}| \langle \rangle \left(\frac{1}{m_q} - \frac{2}{\tilde{M}_X} - \frac{m_b m_q}{\tilde{M}_X^2 \mu_-} \right) \right], \quad (\text{E21})$$

$$b_- = \frac{\tilde{M}_X^2}{2|\mathbf{q}|^2 \tilde{M}_B^2} \left[\langle p_z \rangle \left(\frac{1}{\mu_+} - \frac{(\tilde{M}_X + \tilde{M}_B)}{2m_b m_q} \right) - \langle p_+ \rangle \left(\frac{1}{\mu_+} - \frac{(\tilde{M}_X + \tilde{M}_B)}{2m_b m_q} \right) + |\mathbf{q}| \langle \rangle \left(\frac{1}{m_q} - \frac{2}{\tilde{M}_X} + \frac{(\tilde{M}_B + \tilde{M}_X)}{\tilde{M}_X^2} \right) \right]. \quad (\text{E22})$$

APPENDIX F: DECAY CONSTANTS IN THE QUARK MODEL

A non relativistic quark model calculation using simple harmonic oscillator wavefunctions gives:

$$f_{1P_0} = i\sqrt{2} \frac{N(Y)}{M_Y}, \quad (\text{F1})$$

$$f_{1P_1} = \sqrt{2} \frac{N(Y)}{M_Y}, \quad (\text{F2})$$

$$f_{3P_0} = -i\sqrt{3} \frac{\beta_Y N(Y)}{\mu_- M_Y}, \quad (\text{F3})$$

$$f_{3P_1} = -\sqrt{2} \frac{\beta_Y N(Y)}{\mu_+ M_Y}, \quad (\text{F4})$$

$$f_{1P_1} = \frac{\beta_Y N(Y)}{\mu_- M_Y}, \quad (\text{F5})$$

$$f_{3P_2} = 0. \quad (\text{F6})$$

β_Y is the SHO wavefunction parameter,

$$N(Y) \propto (4\pi\beta_Y^2)^{\frac{3}{4}} \sqrt{M_Y}$$

and

$$\frac{1}{\mu_{\pm}} = \frac{1}{m_{q2}} \pm \frac{1}{m_{q1}}.$$

For general wavefunctions the above equations are replaced by:

$$f_{1P_0} = i\sqrt{2} \frac{N(Y)}{M_Y} \langle 0, 0 | 0 \rangle_L, \quad (\text{F7})$$

$$f_{1P_1} = \sqrt{2} \frac{N(Y)}{M_Y} \langle 0, 0 | 0 \rangle_L, \quad (\text{F8})$$

$$f_{3P_0} = -i \frac{1}{\sqrt{6}} \frac{N(Y)}{\mu_- M_Y} (\langle 1, 0 | p_z | 0 \rangle_L + \langle 1, 1 | p_+ | 0 \rangle_L + \langle 1, -1 | p_- | 0 \rangle_L), \quad (\text{F9})$$

$$f_{3P_1} = -\frac{1}{2} \frac{N(Y)}{\mu_+ M_Y} (\langle 1, 1 | p_+ | 0 \rangle_L + \langle 1, -1 | p_- | 0 \rangle_L), \quad (\text{F10})$$

$$f_{1P_1} = \frac{1}{\sqrt{2}} \frac{N(Y)}{\mu_- M_Y} \langle 1, 0 | p_z | 0 \rangle_L, \quad (\text{F11})$$

$$f_{3P_2} = 0. \quad (\text{F12})$$

Here the overlaps $\langle l, m_l | p_i | 0 \rangle_L$ only contain the *spatial* integrals; the spin and Clebsh-Gordan factors have already been taken care of. $p_+ = -\frac{1}{\sqrt{2}}(p_x + ip_y)$ and $p_- = \frac{1}{\sqrt{2}}(p_x - ip_y)$.

Note that a tensor meson can not be produced from

an axial-vector current.

In the equal mass limit $\frac{1}{\mu_-} = 0$ and so the scalar or 1P_1 axial can not be produced. However, the 3P_1 axial can be produced.

In the heavy quark limit where the quark mass $m_A \rightarrow \infty$ and $\mu_- = \mu_+$ both axial vectors can be produced. It

is useful to change from the L-S basis $^{2s+1}L_J$ to the j-j coupling basis $^jJ^P$ where j is the total angular momentum of the light degrees of freedom, J is the total angular momentum and P is the parity. The transformation is given by [29]:

$$|{}^1P_1\rangle = \sqrt{\frac{1}{3}}|{}^{1/2}1^+\rangle + \sqrt{\frac{2}{3}}|{}^{3/2}1^+\rangle \quad (\text{F13})$$

$$|{}^1P_1\rangle = -\sqrt{\frac{2}{3}}|{}^{1/2}1^+\rangle + \sqrt{\frac{1}{3}}|{}^{3/2}1^+\rangle \quad (\text{F14})$$

$$|{}^{3/2}1^+\rangle = \sqrt{\frac{2}{3}}|{}^1P_1\rangle + \sqrt{\frac{1}{3}}|{}^3P_1\rangle \quad (\text{F15})$$

$$|{}^{1/2}1^+\rangle = \sqrt{\frac{1}{3}}|{}^1P_1\rangle - \sqrt{\frac{2}{3}}|{}^3P_1\rangle \quad (\text{F16})$$

In the heavy quark limit $f_{^3P_1} = -\sqrt{2}f_{^1P_1}$ and so:

$$f_{^{3/2}1^+} = 0, \quad (\text{F17})$$

$$f_{^{1/2}1^+} = \sqrt{3}f_{^1P_1}, \quad (\text{F18})$$

$$f_{^{1/2}0^+} = -i\sqrt{3}f_{^1P_1}. \quad (\text{F19})$$

So the ${}^{3/2}1^+$ axial can not be produced but the ${}^{1/2}1^+$ axial can. Note also that, apart from a phase, the scalar has the same decay constant. This is a specific realisation of the general result given by Le Yaouanc et. al. in Ref. [29].

It is important to note that if it was the *antiquark* mass that was large there would be a relative negative sign between μ_- and μ_+ which would change the negative signs around in the basis change between L-S and j-j coupling. This means that the basis transformation has different signs in D_s^+ and D_s^- mesons.